NeuroImage 70 (2013) 150–163

Contents lists available at SciVerse ScienceDirect

NeuroImage

journal homepage: www.elsevier.com/locate/ynimg

Thalamo-cortical mechanisms underlying changes in amplitude and frequency of human alpha oscillations

Rikkert Hindriks [a,c,*], Michel J.A.M. van Putten [a,b]

[a] Department of Clinical Neurophysiology, MIRA-Institute for Biomedical Technology and Technical Medicine, University of Twente, 7500 AE Enschede, The Netherlands
[b] Department of Neurology and Clinical Neurophysiology, Medisch Spectrum Twente, Enschede, The Netherlands
[c] Center for Brain and Cognition, Computational Neuroscience Group, Department of Information and Communication Technologies, Universitat Pompeu Fabra, Barcelona, 08018, Spain

ARTICLE INFO

Article history:
Accepted 8 December 2012
Available online 21 December 2012

Keywords:
EEG
Alpha oscillations
Thalamo-cortical system
Neural masses

ABSTRACT

Although a large number of studies have been devoted to establishing correlations between changes in amplitude and frequency of EEG alpha oscillations and cognitive processes, it is currently unclear through which physiological mechanisms such changes are brought about. In this study we use a biophysical model of EEG generation to gain a fundamental understanding of the functional changes within the thalamo-cortical system that might underly such alpha responses. The main result of this study is that, although the physiology of the thalamo-cortical system is characterized by a large number of parameters, alpha responses effectively depend on only three variables. Physiologically, these variables determine the resonance properties of feedforward, cortico-thalamo-cortical, and intra-cortical circuits. By examining the effect of modulations of these resonances on the amplitude and frequency of EEG alpha oscillations, it is established that the model can reproduce the variety of experimentally observed alpha responses, as well as the experimental finding that changes in alpha amplitude are typically an order of magnitude larger than changes in alpha frequency. The modeling results are also in line with the fact that alpha responses often correlate linearly with indices characterizing cognitive processes. By investigating the effect of synaptic and intrinsic neuronal parameters, we find that alpha responses reflect changes in cortical activation, which is consistent with the hypothesis that alpha activity serves to selectively inhibit cortical regions during cognitive processing demands. As an example of how these analyses can be applied to specific experimental protocols, we reproduce benzodiazepine-induced alpha responses and clarify the putative underlying thalamo-cortical mechanisms. The findings reported in this study provide a fundamental physiological framework within which alpha responses observed in specific experimental protocols can be understood.

Introduction

The most dominant characteristic of electro-encephalographic (EEG) recordings in awake human subjects is alpha oscillation, which refers to periodic fluctuations within the frequency band of 8–13 Hz. Since the first human EEG recordings performed by Hans Berger more than eighty years ago (Berger, 1929), an enormous number of studies have been devoted to establishing correlations between cognitive processes and characteristics of alpha oscillations, in particular changes in their amplitude and frequency, which we will further refer to as *alpha responses*. The diversity of such studies is large and includes manipulation with pharmacological substances such as propofol and thiopental (Feshchenko et al., 2004), nicotine (Domino et al., 2009; Roth, 1991), ethanol (Lukas et al., 1990), MDMA (Dafters et al., 1999), and THC (Volavka et al., 1973), psychiatric, psychological, and neurological syndromes such as schizophrenia (Merrin and Floyd, 1996), attention deficit hyperactivity disorder (ADHD) (Koehler et al., 2009), depression (Gotlib, 1998), mania (Flor-Henry and Koles, 1984), autism (Cantor et al., 1986), and Alzheimer's disease (Kuskowski et al., 1993; Moretti, 2004), as well as emotional and arousal states (Banquet, 1973; Knyazev et al., 2004; Kostyunina and Kulikov, 1996). In such and similar studies, correlations are established between cognitive variables and alpha responses as measured with EEG. In addition to these resting-state paradigms, different lines of research have studied human alpha oscillations during specific cognitive tasks and the presentation of controlled stimuli (ERS/ERD). These task-related paradigms allow for a more specific mapping between cognitive processes and alpha oscillations, thereby allowing hypothesis to be formulated regarding their role in cognition and perception (Jensen et al., 2002; Klimesch et al., 1998; Pfurtscheller et al., 1996). Although such empirical studies as the ones mentioned above establish correlations (and in some cases causal links; Hummel et al., 2002) between cognitive processes and alpha oscillations, by themselves they are incapable of pinpointing the physiological mechanisms through which the observed changes in alpha amplitude and frequency are brought about.

Currently, there is no consensus regarding the physiological mechanisms underlying the generation of human alpha oscillations. While

* Corresponding author.
E-mail address: rikkert.hindriks@upf.edu (R. Hindriks).

1053-8119/$ – see front matter © 2013 Elsevier Inc. All rights reserved.
http://dx.doi.org/10.1016/j.neuroimage.2012.12.018

some theories stress the importance of intrinsic membrane properties of particular neurons and propose that alpha oscillations are generated by intrinsic rhythmic properties of these neurons, other theories stress the importance of synaptic connections and claim that alpha oscillations emerge from network properties of thalamic (Lopes da Silva et al., 1974) or cortical tissue (Liley and Cadusch, 2002; Nunez, 1989; Nunez, 1974; van Rotterdam and Lopes Da Silva, 1982), or from reverberation within thalamo-cortical feedbacks loops (Rennie et al., 2002; Robinson et al., 2001, 2002). Neuroimaging studies show the existence of correlations between metabolic rates and alpha amplitudes both in cortical as well as in diverse subcortical structures (Sadato et al., 1998), in particular the thalamus (Goldman et al., 2002; Gonçalves et al., 2006; Larson et al., 1998; Schreckenberger et al., 2004). These results show that the functional states of thalamic nuclei are related to alpha amplitudes and suggest that they play a role in either the generation or modulation of alpha oscillations. A recently developed biophysical model of the EEG that makes explicit the thalamo-cortico-thalamic reverberation hypothesis of alpha generation is described in Rennie et al. (2002) and Robinson et al. (2001, 2002). Besides displaying spontaneous alpha oscillations, the model provides an integrated explanation of such diverse EEG phenomena as spontaneous oscillations within different frequency bands, both during wakefulness as well as during sleep (Robinson et al., 2001), event-related potentials (Rennie et al., 2002), and the generation of some of the generalized epilepsies (Breakspear et al., 2006). In this study we employ this model to obtain insight into the thalamo-cortical mechanisms presumably underlying alpha responses observed in EEG experiments.

Although all of the above mentioned empirical studies observe changes in the amplitude and frequency of ongoing alpha oscillations, the physiological causes that are responsible for the observed changes depend on the specific experimental paradigm. Several drugs and pharmacological agents modulate EEG rhythms, including the alpha rhythm. Examples include ethanol and anesthetic agents as propofol, that have strong affinity for the $GABA_A$ receptors in the cortex and thalamus, resulting in dose-dependent effects of both the amplitude and frequency of the alpha rhythm (Feshchenko et al., 2004; Kuizenga et al., 2001). There are many cholinergic pathways in the human brain and the endogenous neurotransmitter acetylcholine has various effects on the alpha rhythm too (Steriade et al., 1990). As the muscarinic or nicotinic acetylcholine receptors are expressed differently in various populations of interneurons, both in cortex and thalamus, a rich phenomenology of modulations of the alpha rhythm seems possible. Indeed, nicotine is reported to increase the dominant alpha frequency (Domino et al., 2009; Roth, 1991). Centrally acting anticholinesterase inhibitors, e.g. donepezil or rivastigmine, approved to treat patients with Alzheimer disease, have been shown to increase centroparietal alpha power during REM sleep (Moraes et al., 2006). Also, during normal aging different effects on muscarinic and nicotinic receptor subtypes were observed in postmortem brain tissue from different regions of the human brain (Nordberg et al., 1992), which may be responsible for the small, but significant decline in the dominant alpha frequency during aging (Lodder and van Putten, 2011). Furthermore, although in general, the physiological processes involved in cognitive processing and psychiatric and mood disorders are not known in detail, they most likely involve several neuromodulatory systems and receptor types with complex interactions.

Complete understanding of the detailed physiological changes underlying alpha responses therefore, requires—in addition to a computational model of the generation of EEG alpha oscillations—detailed physiological mechanisms that are specific to the experimental paradigm that is used to invoke the observed responses. In this study we pursue a more generic approach by determining which features of the thalamo-cortical system determine experimentally observed alpha responses. The assumption underlying this approach is that the physiological changes induced by experimental paradigms, change alpha frequency and amplitude by modulating the functional state of the thalamo-cortical system. Alpha responses are then a direct reflection of this altered functionality. Thus, although the specific physiological changes underlying the alpha responses are left implicit, this approach makes explicit the thalamo-cortical correlates underlying alpha responses that might be common to different experimental protocols.

In the Introduction and Materials and methods sections we provide a description of the thalamo-cortical model of the EEG and the associated theoretical EEG power spectrum, respectively. In the Introduction we show that alpha responses are induced by the non-linear membrane properties of the different neuron types within the thalamo-cortical system and that they are determined by modulations of the resonance properties of the feedforward, thalamo-cortico-thalamic circuits. In the Materials and methods section we investigate the differential effects of modulations in the resonance properties of these circuits. In the Results section we inventarize the effects of changes in synaptic and intrinsic neuronal parameters and analyze through which resonance-modulations the induced alpha responses are brought about. We also apply the methodology to alpha responses induced by administration of benzodiazepines and investigate the underlying thalamo-cortical mechanisms. In the Discussion section we discuss the main findings of this study, its limitations, and possible directions for further research.

Materials and methods

In this section we introduce the ingredients that we will use in the Results section to investigate the physiological mechanisms underlying alpha responses, which is the main focus of this study. Specifically, in the Thalamo-cortical model of EEG generation section we introduce the thalamo-cortical model of EEG generation (Rennie et al., 2002; Robinson et al., 2001). This includes the specification of the different types of neuronal populations comprising the thalamo-cortical circuitry together with their activation properties, the synaptic responses and the corresponding synaptic impacts, as well as the dynamics governing the spreading of neuronal activation over the cortical sheet. In the Theoretical EEG power spectrum section we introduce the theoretical EEG power spectrum, which is derived from linearizing the model equations about a stable equilibrium state. The power spectrum will be expressed in terms of neuronal excitabilities and synaptic frequency responses, which will be defined in the same subsection. In addition, we describe how responses in frequency and amplitude are quantified in this study.

Thalamo-cortical model of EEG generation

In Robinson et al. (2001) and Rennie et al. (2002) a computational model of the generation of EEG rhythms is developed. In contrast to network models, which describe the electrochemical properties of neuronal tissue by simulating large numbers of synaptically coupled neurons, the model developed in Robinson et al. (2001) and Rennie et al. (2002) describes the *average behavior* of such networks. Thus, rather than tracking the behavior of the membrane potentials of a large number of individual neurons, the model captures the average potential dynamics of populations of neurons. This approach therefore, is *macroscopic* hence naturally connects with the EEG, which is a macroscopic signal, reflecting the total synaptic current into large numbers of cortical pyramidal neurons.

The model comprises four types of neuronal populations, namely, cortical pyramidal neurons, cortical inhibitory neurons, thalamic reticular neurons, and thalamo-cortical relay neurons, whose *average membrane potentials* are denoted by V_k, for $k \in \{e,i,r,s\}$, respectively. The synaptic organization of these neuronal populations is illustrated in Fig. 1. Synaptic transmission from neurons of type l to neurons of type k is modeled by a function $h_{kl}(t)$ called the *synaptic response*, which is defined by

$$h_{kl}(t) = \frac{\rho_{kl}}{c_{kl}}[\exp(-\alpha_{kl}t) - \exp(-\beta_{kl}t)], \quad (1)$$

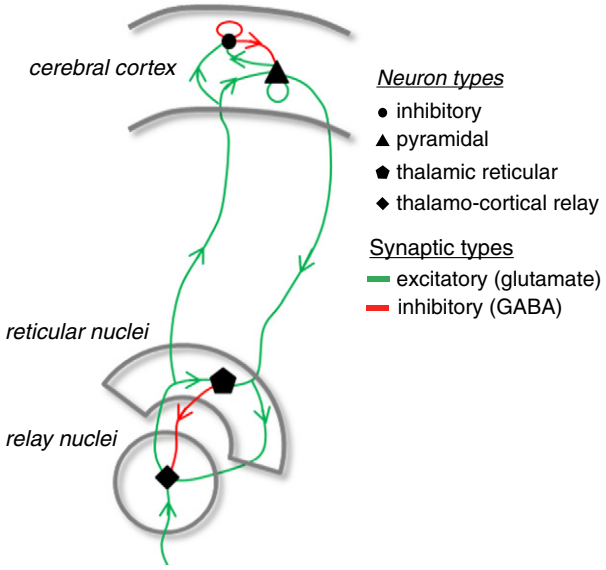

Fig. 1. Synaptic organization of the thalamo-cortical model. Illustrated are the synaptic pathways that connect the different neuronal populations. The model contains four types of neuronal populations, consisting of cortical pyramidal neurons and interneurons, thalamo-cortical relay neurons and thalamic reticular neurons, which are connected through excitatory (AMPA/NMDA) and inhibitory (GABA) synaptic projections.

where ρ_{kl} is called the *synaptic efficacy* and where β_{kl} and α_{kl} are the *synaptic rise- and decay-rates*, respectively, which typically satisfy $\beta_{kl}>\alpha_{kl}$ (Robinson et al., 1997). The normalization constant c_{kl} depends on α_{kl} and β_{kl} and is chosen such that the maximum value of h_{kl} equals ρ_{kl}. The synaptic response is illustrated in Fig. 2(A).

The synaptic efficacy can be written as $\rho_{kl}=N_{kl}s_{kl}$, where N_{kl} is the number of synaptic contacts on neurons of type k originating from neurons of type l, and s_{kl} is the synaptic efficacy of an individual synapse. Excitatory synaptic transmission is modeled by positive efficacies and inhibitory synaptic transmission is modeled by negative efficacies. Thus, $\rho_{kl}>0$ for $l\in\{e,s\}$ and $\rho_{kl}<0$ for $l\in\{i,r\}$. A variable that is of physiological interest in characterizing synaptic transmission and that will be used in subsequent sections is the *synaptic impact*, which we denote by λ_{kl} and is defined as

$$\lambda_{kl}=\int_0^\infty h_{kl}(t)dt. \tag{2}$$

The synaptic impact is proportional to the total post-synaptic current summed over all N_{kl} synaptic contacts.

The average membrane potential at time t, $V_k(t)$ and the *average firing-rate* $Q_k(t)$, with unit s^{-1}, are related via $Q_k(t)=S_k(V_k(t))$, where S_k is the *neuronal activation function*, defined as

$$S_k(V_k)=\frac{Q_k^{\max}}{1+\exp(-(V_k-\theta_k)/\sigma_k)}, \tag{3}$$

where $Q_k^{\max}$, θ_k, and σ_k denote the *maximal firing-rate*, *average spike-threshold* in mV, and the dispersion of activation thresholds over the neural population of type k, respectively. The parameters $Q_k^{\max}$, θ_k are population averages and arise from the intrinsic membrane properties of the different types of neurons. Table 1 lists all model variables, together with their symbols and units. The membrane potentials have a resting-value of 0 mV and the spike-thresholds are chosen relative to this resting-value. Fig. 2(B) displays the neuronal activation function with values $Q_k^{\max}=250\,1/s^{-1}$, $\theta_k=15$ mV, and $\sigma_k=3.3$ mV.

The last model ingredient concerns the propagation of firing-rates of pyramidal neurons through long-range cortico-cortical fibers. This

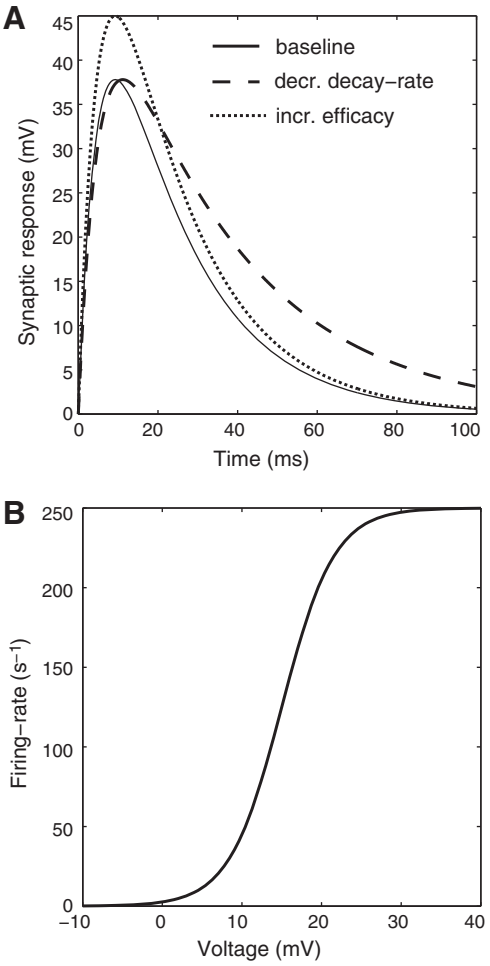

Fig. 2. Synaptic responses and neuronal activation function. (A) Synaptic responses $h(t)$ for three different parameter-settings: baseline for which $\alpha=50\ s^{-1}$, $\beta=200\ s^{-1}$, and $\rho=37.8$ mV (solid line), decreased decay-rate $\alpha=30\ s^{-1}$ (dashed line), and increased efficacy $\rho=45$ mV (dotted line). (B) Neuronal activation function for baseline neuronal parameters: $Q^{\max}=250\ s^{-1}$, $\theta=15$ mV, and $\sigma=3.3$ mV.

propagation is assumed to be isotropic, with constant velocity of v and to obey the following wave equation:

$$\left[\left(\frac{1}{\gamma}\frac{\partial}{\partial t}+1\right)^2-l^2\nabla^2\right]\phi_e(t)=Q_e(t), \tag{4}$$

where ϕ_e is the firing-rate from distant pyramidal populations coming in at time t, l the characteristic axonal length of cortical pyramidal neurons, and $\gamma=v/l$ is the cortical damping rate (Robinson et al., 1997).

Table 1
Model variables, their symbols, and units. All variables are averages over the respective neuronal populations.

Variable	Symbol	Unit
Membrane potential of pyramidal neurons	V_e	mV
Membrane potential of interneurons	V_i	mV
Membrane potential of thalamic reticular neurons	V_r	mV
Membrane potential of thalamo-cortical relay neurons	V_s	mV
Firing-rate of pyramidal neurons	Q_e	s^{-1}
Firing-rate of interneurons neurons	Q_i	s^{-1}
Firing-rate of thalamic reticular neurons	Q_r	s^{-1}
Firing-rate of thalamo-cortical relay neurons	Q_s	s^{-1}
Incoming firing-rate of pyramidal neurons	ϕ_e	s^{-1}
Incoming non-specific firing-rate	ϕ_n	s^{-1}

Following Hindriks and van Putten (2012) and Robinson et al. (2002) we set $\nabla^2 = 0$, thereby restricting to spatially-homogeneous dynamics of ϕ_e on the cortex. The EEG signal is modeled by ϕ_e since these are approximately proportional (Rennie et al., 2002; Robinson et al., 1997). The equations governing the models' dynamics are described in Appendix A. We use the nominal parameter values from Robinson et al. (2002) displayed in Table 2 as the baseline condition, since they were previously identified with eyes-closed alert wakefulness (Rennie et al., 2002) which is often chosen as the baseline condition in experimental studies on alpha responses. The model parameters are denoted by the vector p and the baseline parameter values are denoted by p_0. In Fig. 3(A) a numerically simulated EEG time-series in baseline is displayed and Fig. 3(B) shows its theoretical power spectrum, which we consider in the next section.

Theoretical EEG power spectrum

Time-series analyses have shown that human EEG alpha oscillations are dominated by linear dynamics (Stam et al., 1999) and reflect fluctuations about an equilibrium-state (Hindriks et al., 2011). Within the present modeling context, this means that their dynamics can be studied by performing a linearization of the model equations, which allows for an explicit mathematical expression of the associated EEG power spectrum. Let V_k^* for $k=\{e,i,r,s\}$ be a stable equilibrium-state. Since the neuronal activation functions S_k are the only non-linear terms in the model equations, a linearization of these equations is obtained by linearizing S_k about V_k^*:

$$S_k(V_k) \approx S_k(V_k^*) + \frac{d}{dV} S_k(V_k^*)(V_k - V_k^*), \tag{5}$$

where the derivative is taken with respect to voltage V. A quantity that will be important for characterizing alpha responses is the *neuronal excitability*, denoted by ϵ_k and defined as

$$\epsilon_k = \frac{d}{dV} S_k(V_k^*). \tag{6}$$

It measures the change in the firing-rate of the neuronal population of type k induced by a perturbation in its membrane voltage, when the population's membrane potential is close to its equilibrium-state V_k^*. Before we state the mathematical expression for the theoretical EEG power spectrum, we introduce the *frequency response*, denoted by L_{kl} and which is defined as the Fourier transformation of the synaptic response h_{kl}:

$$L_{kl}(\omega) = \frac{\rho_{kl}/c_{kl}}{(\alpha_{kl}+\omega)(\beta_{kl}+\omega)}, \tag{7}$$

where ω denotes angular frequency.

Using the notation $\delta_{kl}(\omega) = L_{kl}(\omega)$, in Appendix B it is derived that the theoretical EEG power spectrum is given by

$$P_{EEG}(\omega) = \frac{\sigma_n^2 |X(\omega)|^2}{|2i\omega/\gamma - \omega^2/\gamma^2 + Y(\omega) - Z(\omega)e^{-i\omega\tau}|^2}, \tag{8}$$

where

$$X(\omega) = \frac{(1-\delta_{ii})\delta_{esn} + \delta_{eisn}}{(1-\delta_{ii})(1-\delta_{srs})}, \tag{9}$$

$$Y(\omega) = \frac{(1-\delta_{ee})(1-\delta_{ii}) - \delta_{eie}}{1-\delta_{ii}}, \tag{10}$$

and

$$Z(\omega) = \frac{(1-\delta_{ii})(\delta_{ese}+\delta_{esre}) + \delta_{eise} + \delta_{eisre}}{(1-\delta_{ii})(1-\delta_{srs})}, \tag{11}$$

where we have suppressed the dependence of δ_{kl} on ω. In the above expression, the δ_{kl}s have been combined. Thus, for example $\delta_{srs} = \epsilon_s \epsilon_r L_{srs}$, where $\epsilon_s \epsilon_r$ and $L_{srs} = L_{sr}L_{rs}$ denote, respectively, the excitability and frequency response of the intra-thalamic loop. In general we use the index $M \in \{ee, ii, eie, ese, esre, eise, eisre, srs, esn, eisn\}$ to refer to the different anatomical loops and feedforward pathways. The complex-valued functions $X(\omega)$, $Y(\omega)$, and $Z(\omega)$, characterize the resonance properties of cortical pyramidal neurons when embedded in the feedforward, intra-cortical, and cortico-thalamo-cortical circuits, respectively. Fig. 4 illustrates the synaptic organization of these circuits. In Appendix C we describe the relation between these variables and the coordinates used in Robinson et al. (2002) to map the linear stability boundary of a more specific version of the currently used model.

Alpha frequencies and amplitudes are calculated by numerically computing the peak-amplitude $A(p)$ and peak-frequency $F(p)$ of the

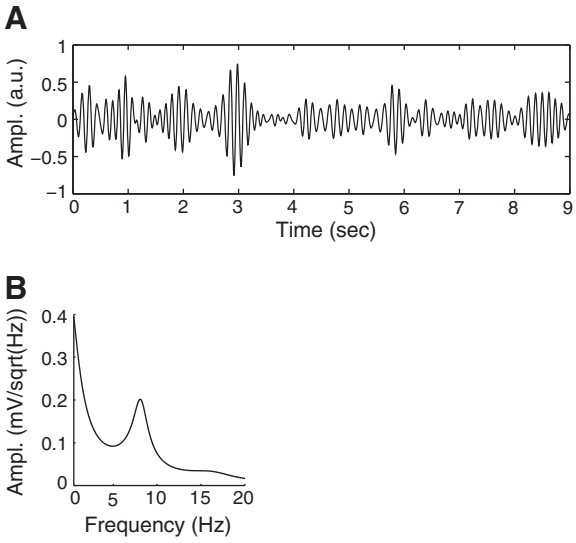

Fig. 3. Simulated EEG alpha oscillations in baseline. (A) numerical simulation of the model equations using the baseline parameters values (see Table 2). The signal was bandpass filtered between 6 and 10 Hz (the alpha peak-frequency in baseline is about 8 Hz). (B) Corresponding broadband theoretical power spectrum calculated from Eq. (8).

Table 2
Model parameters, their symbols, and nominal values[a]. The subscripts k, l $\{e,i,r,s\}$ refer to the different neuron types and the double subscript kl refers to synaptic connections from neurons of type l to neurons of type k.

Parameter	Symbol	Nominal value
Maximal firing-rate	Q_k^{max}	250 s^{-1}
Average spike-threshold	θ_k	15 mV
Spike-threshold deviation	σ_k	3.3 mV
Synaptic decay rate	α_{kl}	50 s^{-1}
Synaptic rise rate	β_{kl}	200 s^{-1}
Synaptic efficacy from e to e neurons	ρ_{ee}	37.8 mV
Synaptic efficacy from i to e neurons	ρ_{ei}	−56.7 mV
Synaptic efficacy from s to e neurons	ρ_{es}	37.8 mV
Synaptic efficacy from i to i neurons	ρ_{ii}	−56.7 mV
Synaptic efficacy from e to i neurons	ρ_{ie}	37.8 mV
Synaptic efficacy from s to i neurons	ρ_{is}	37.8 mV
Synaptic efficacy from r to s neurons	ρ_{sr}	−25.2 mV
Synaptic efficacy from e to s neurons	ρ_{se}	37.8 mV
Synaptic efficacy from s to r neurons	ρ_{rs}	6.3 mV
Synaptic efficacy from e to r neurons	ρ_{re}	12.6 mV
Average noise level	$\nu_{sn}\langle\phi_n\rangle$	1 mV
Noise standard deviation	σ_n	0.1 mV
Cortico-thalamic delay	τ	0.08 s
Cortical damping rate	γ	100 s^{-1}

[a] P. Robinson, C. Rennie, and D. Rowe. Dynamics of large-scale brain activity in normal arousal states and epileptic seizures. *Physical Review E*, 65(4):1–9, April 2002.

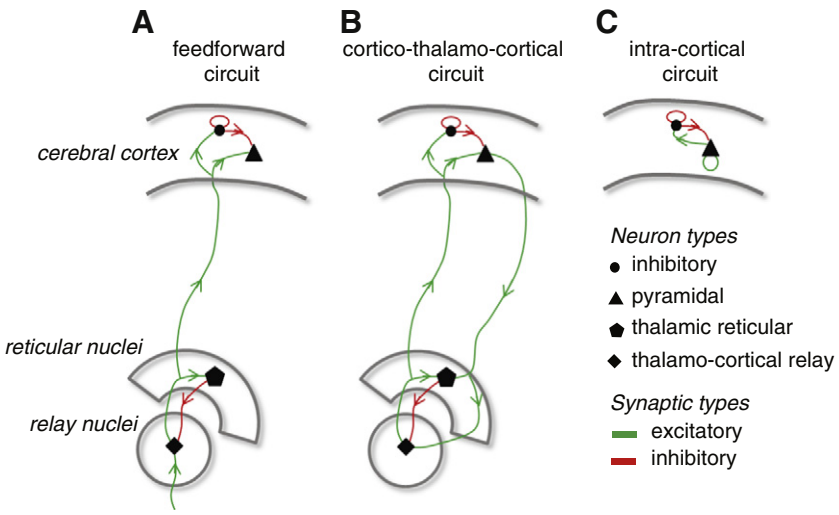

Fig. 4. Circuits comprising the thalamo-cortical system. (A) Feedforward circuit, (B) thalamo-cortico-thalamic circuit, (C) intra-cortical circuit.

theoretical EEG power spectrum (Eq. (8)). Responses in alpha amplitude $\Delta A(p)$ and frequency $\Delta F(p)$ are computed relative to baseline p_0:

$$\Delta A(p) = \frac{A(p) - A(p_0)}{A(p_0)}, \tag{12}$$

and

$$\Delta F(p) = \frac{F(p) - F(p_0)}{F(p_0)}, \tag{13}$$

as illustrated in Fig. 5. We use the expression $\Delta(p)$ to refer to alpha responses in general. In the sequel, we distinguish *positively correlated* and *negatively correlated* alpha responses $\Delta(p)$, which are defined by $\Delta A(p)$ and $\Delta F(p)$ having the same and opposite signs, respectively. We use the term *mono-phasic* to refer to responses in amplitude and frequency that either increase or decrease as a function of p. These are in contrast to responses that display a more complicated profile as a function of p.

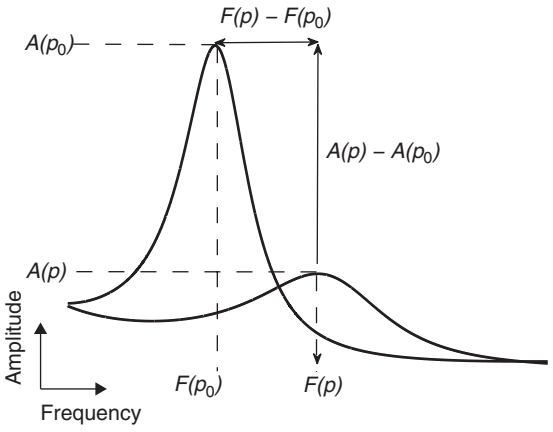

Fig. 5. Relative alpha responses. Shown are illustrations of EEG power spectra in baseline (corresponding to p_0) and one corresponding to p. $F(p_0)$ and $A(p_0)$ denote the peak-frequency and peak-amplitude of the alpha rhythm in baseline, respectively, and $F(p)$ and $A(p)$ denote, respectively, the peak-frequency and peak-amplitude of the alpha rhythm corresponding to the parameter value p. Responses of alpha-amplitude $\Delta A(p)$ and alpha-frequency $\Delta F(p)$ are computed relative to their baseline values $\Delta A(p_0)$ and $\Delta F(p_0)$, respectively.

Results

In this section we investigate the putative thalamo-cortical mechanisms through which alpha responses are brought about. In particular, in the Reduced EEG power spectrum section we argue that as far as alpha responses are concerned, the theoretical EEG power spectrum allows for a reduction which shows that alpha responses effectively depend only on three variables, namely, the resonance properties of the feedforward, thalamo-cortico-thalamic, and intra-cortical circuits at alpha peak frequency. In the Gain and phase modulation of system circuits section we analyze the effects of modulations of these resonances, showing that induce distinct alpha responses. In the Physiological alpha responses section we classify the effects of variations in individual model parameters on alpha frequency and amplitude and characterize the underlying resonance-modulations. In the Benzodiazepine-induced alpha responses section we apply the model to a specific experimental protocol, where we try to reproduce alpha responses induced by the administration of benzodiazepines and clarify the putative underlying mechanisms in terms of resonance modulations of the different thalamo-cortical circuits.

Reduced EEG power spectrum

In order to pinpoint which changes in the functionality of the thalamo-cortical system determine observed changes in the amplitude and frequency of EEG alpha oscillations, it is convenient to divide the model parameters into two groups, namely those that characterize synaptic transmission and those that characterize the activation properties of the neuronal populations. Specifically, synaptic transmission is characterized by the synaptic rate-constants α_{kl} and β_{kl} and the synaptic efficacies ρ_{kl} and neuronal activation is characterized by the maximal firing-rates $Q_k^{\max}$, spike-thresholds θ_k, and the dispersion of spike-thresholds over the populations σ_k.

Eq. (8) shows that alpha responses are induced by modulations in the resonance properties of the feedforward, thalamo-cortico-thalamic, and intra-cortical circuits via changes in the synaptic responses L_{kl} and neuronal excitabilities ϵ_k. The changes in L_{kl} on their turn, are caused by changes in synaptic parameters, as can be seen from Eq. (7), and changes in neuronal excitabilities can be caused by changes in synaptic parameters as well as neuronal activation parameters, but through different mechanisms. The different dependencies are illustrated in Fig. 6. Specifically, changes in synaptic parameters lead to changes in synaptic impacts λ_{kl} (see Eq. (2)), which alter the equilibrium firing-rates of the different neuronal populations as is evident from the equilibrium equations derived in Appendix D. Changes in equilibrium firing-rates on their turn, lead to

excitability changes as can be seen from Eq. (6). In contrast, changes in neuronal activation parameters directly cause excitability changes via Eq. (6) and indirectly, by altering equilibrium firing-rates.

The changes in synaptic parameters that induce alpha responses of the same order of magnitude as those observed experimentally lead to changes in synaptic responses L_{kl} that are much smaller than the alterations in equilibrium firing-rates and contribute only marginally to the induced alpha responses. We have confirmed this by comparing alpha responses induced by variations of $\pm 2\%$ in all synaptic parameters with the corresponding responses resulting from keeping the synaptic responses fixed to baseline. This allows us to make the following approximation:

$$L_{kl}\left(\omega|\alpha_{kl},\beta_{kl},\rho_{kl}\right)\approx L_{kl}\left(\omega\middle|\alpha_{kl}^0,\beta_{kl}^0,\rho_{kl}^0\right). \tag{14}$$

This approximation shows that the modulations in $X(\omega)$, $Y(\omega)$, and $Z(\omega)$ effectively depend only on changes in the excitabilities ϵ_k of the different neuronal types. Physiologically, this means that alpha responses reflect changes in non-linear neuronal activation properties.

Further reduction of the effective physiology underlying alpha responses is based on the observation that for frequencies ω close to the alpha baseline frequency ω_α, the approximation

$$L_{kl}\left(\omega\middle|\alpha_{kl}^0,\beta_{kl}^0,\rho_{kl}^0\right)\approx L_{kl}\left(\omega_\alpha\middle|\alpha_{kl}^0,\beta_{kl}^0,\rho_{kl}^0\right). \tag{15}$$

leaves the EEG power spectrum intact and does not essentially alter alpha responses. Again, we have confirmed this by comparing the respective alpha responses. These approximations allow us to substitute $L_{kl}(\omega_\alpha|\alpha_{kl}^0,\beta_{kl}^0,\rho_{kl}^0)$ for $L_{kl}(\omega|\alpha_{kl},\beta_{kl},\rho_{kl})$ in the expressions for $X(\omega)$, $Y(\omega)$, and $Z(\omega)$. Since $X(\omega)$, $Y(\omega)$, and $Z(\omega)$ are now independent of frequency, we will simply write X, Y, and Z.

Since X, Y, and Z are complex-valued constants, we write them as $X = G_X e^{-i\phi_X}$, where G_X and ϕ_X denote the *gain* and *phase*, respectively of X, and similarly for Y and Z. The gains and phases of X, Y, and Z characterize the resonance properties of cortical pyramidal neurons at alpha baseline frequency ω_α, when embedded in the feedforward, cortico-thalamo-cortical, and intra-cortical circuit, respectively. Specifically, the gains quantify the attenuation of resonant activity at frequency ω_α in the respective circuits and the phases quantify the phase-shift in the respective circuits at frequency ω_α, where a value of 2π corresponds to a delay equal to the mean period of baseline alpha oscillations ($2\pi/\omega_\alpha s$).

The EEG power spectrum can be re-written in terms of the gains and phases of the feedforward, thalamo-cortico-thalamic, and intra-cortical circuits as

$$P_{EEG}(\omega)=\frac{\sigma_n^2 G_X^2}{|2i\omega/\gamma-\omega^2/\gamma^2+G_Y\exp-i\phi Z-G_Z\exp-i(\phi_Z+\tau\omega)|^2}, \tag{16}$$

which shows that alpha responses are effectively determined by modulations in the gains and phases of these circuits at the alpha baseline frequency. In Robinson et al. (2002), the authors study low-frequency EEG oscillations by approximating $L_{kl}\approx 1$, for which X, Y, and Z become real-valued. This approximation however, is valid only for low frequencies and employing it in the current context leads to essentially different alpha responses, which we have checked by comparing the respective responses. Thus, both the gains as well as the phases of the feedforward, cortico-thalamo-cortical, and intra-cortical circuits contribute to alpha responses.

Gain and phase modulation of system circuits

In this section we determine the effects of modulation of the resonance properties of the feedforward, cortico-thalamo-cortical, and intra-cortical circuits on the amplitude and frequency of spontaneous alpha oscillations. As discussed in the Introduction section, such modulations can result from alterations in the dynamics of nervous system structures not explicitly incorporated in the currently used thalamo-cortical model. Since induced alpha responses depend on the exact values of the circuit gains and phases in baseline, we employ a numerical analysis. Specifically, we individually vary the gains by $\pm 50\%$ from their baseline values by multiplying them with a factor that ranges between 0.5 and 1.5. The phases are varied by adding phases that range between $-\pi/4$ and $+\pi/4$. These variations induce responses in alpha amplitude and phase that are of the same order of magnitude as experimentally induced alpha responses. The results are displayed in Fig. 7 and summarized in Table 3. Note that alpha responses can be both positively as well as negatively correlated, which shows that Eq. (16) is flexible enough to reproduce experimentally observed responses (Banquet, 1973; Feshchenko et al., 2004; Volavka et al., 1973). Furthermore, Fig. 7 shows that alpha responses induced by modulation of the resonance properties of individual circuits are mono-phasic, which is in line with experimentally induced amplitude and frequency responses, which typically either increase or decrease as a function of cognitive and pharmacological indices (Dafters et al., 1999; Feshchenko et al., 2004; Jensen et al., 2002; Knyazev et al., 2004; Kuskowski et al., 1993). The figure also shows that frequency responses are an order of magnitude smaller than amplitude responses, in agreement with experimental studies which typically report frequency responses smaller than 20% (Banquet, 1973; Domino et al., 2009; Feshchenko et al., 2004; Kostyunina and Kulikov, 1996; Moretti, 2004; Roth, 1991; Volavka et al., 1973), while amplitude responses are often much larger (Banquet, 1973; Jensen et al., 2002; Klimesch et al., 2007; Knyazev et al., 2004; Koehler et al., 2009). Specifically, modulations in ϕ_Z can change the term $\phi_{Z+\tau\omega}$ by a maximal value of 2π. Therefore, since ω_α is largely determined by this last term, modulation of (combinations of) circuit resonances can shift ω_α by a maximal value of $\approx 2\pi$. This implies that experimentally observed frequency responses larger than ≈ 1 Hz are partly caused by changes in cortical damping rate γ or delay within the thalamo-cortico-thalamic loop τ. The most plausible interpretation is that, during such low- and high-frequency alpha activity, slower and faster axons, respectively, dominate the reverberant activity within the cortico-thalamo-cortical loop.

Table 3 shows that modulation of the phase ϕ_X of the feedforward circuit does not induce an alpha response and the modulation of its gain G_X induces a linear amplitude response, which is also evident from Eq. (16). Thus modulation of the resonance properties of the feedforward circuit cannot induce alpha frequency responses. Also, modulations of the resonance properties of the cortico-thalamo-cortical and inter-cortical circuits induce essentially different alpha responses, Specifically, while modulation of G_Z or ϕ_Y induces a positively correlated response, modulation of G_Y or ϕ_Z induces a negatively correlated response. Lastly, observe that alpha frequency is most sensitive to modulations in the phase ϕ_Z of the intra-cortical circuit and that this alpha dependence is linear, which is also evident from Eq. (16).

Physiological alpha responses

In this section we consider alpha responses induced by variations in individual parameters of the thalamo-cortical system (see Table 2). In experimental settings, alpha responses are typically induced by coordinated changes in several parameters, for example in all glutamatergic or GABAergic receptors throughout the thalamo-cortical system. To gain a basic understanding, however, we restrict to alpha responses induced by changes in individual parameters. Conceptually, it is convenient to divide the model parameters p into two groups, namely those that either promote firing of excitatory neuronal populations (cortical pyramidal neurons (e) and thalamo-cortical relay neurons (s)) or obstruct firing of inhibitory neuronal populations (cortical inhibitory neurons (i) and thalamic relay neurons (r)) and those that either promote firing of inhibitory neuronal populations or obstruct firing of excitatory neuronal

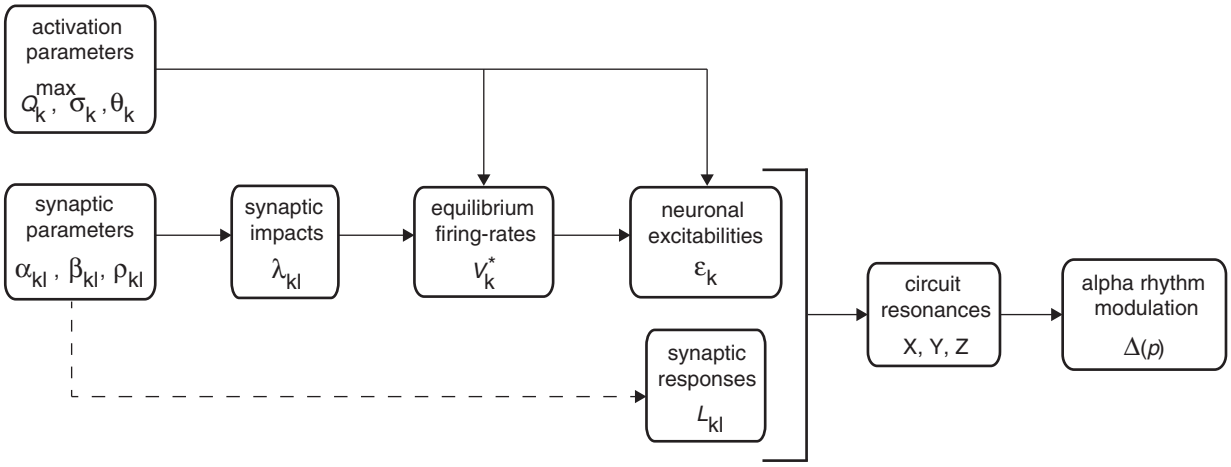

Fig. 6. Parameter-dependencies of alpha responses. The figure illustrates that variations in synaptic and neuronal activation parameters induce alpha responses through different mechanisms. Variations in activation parameters lead to altered neuronal excitabilities, both direct and indirect via changes in equilibrium firing-rates. Variations in synaptic parameters induce alpha responses by altering synaptic impacts λ_{kl}, which alter equilibrium firing-rates, and hence excitabilities. In addition, they also modify synaptic frequency responses.

populations. We denote these groups by p_+ and p_-, respectively. Since uni-directional changes in p_+ and p_- lead to increased and decreased equilibrium firing-rates of cortical pyramidal neurons, respectively, together they characterize the level of cortical activation.

Although parameter variations can be bi-directional, we only consider parameter variations in one direction since we have observed that the resulting alpha responses are mono-phasic. Specifically, we vary p_+ in the direction that increases the firing-rates of excitatory

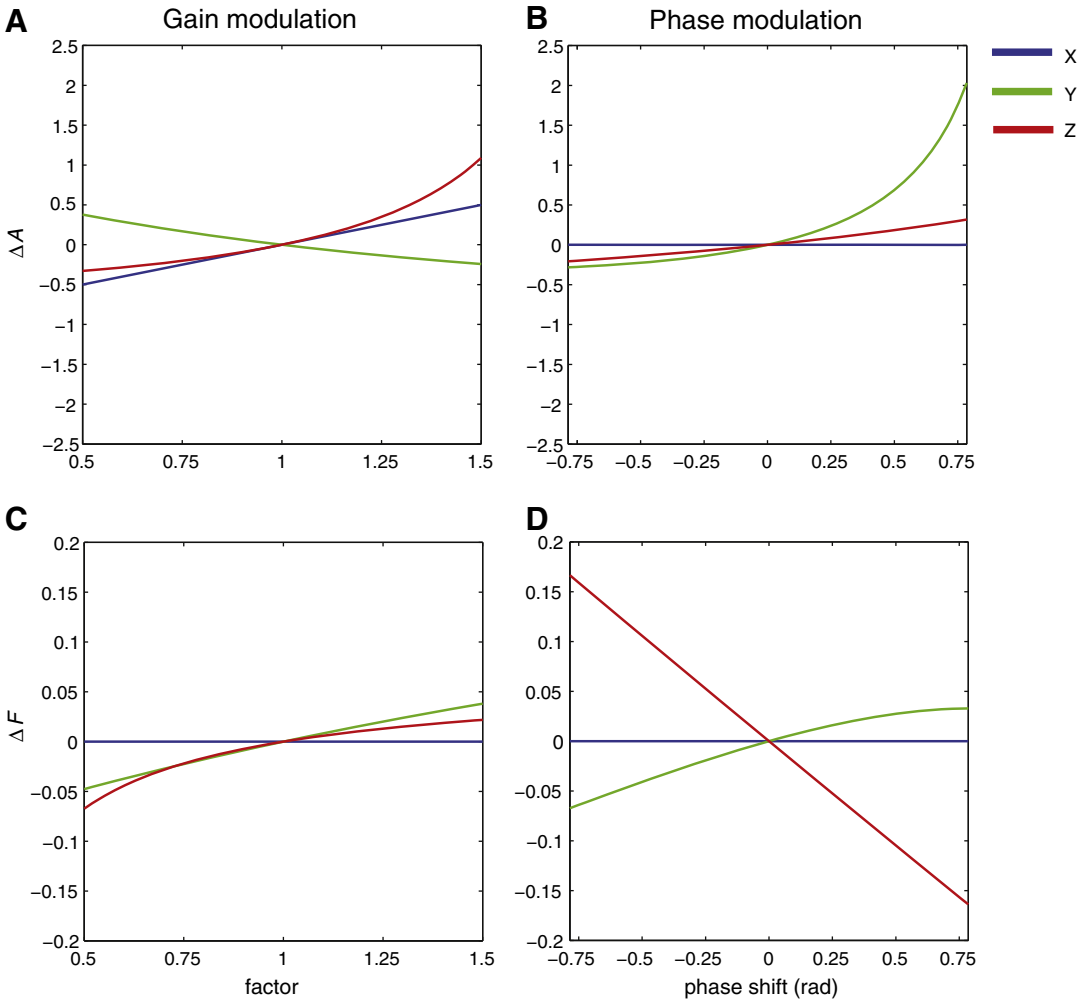

Fig. 7. Effects of resonance modulations in system circuits. Shown are the relative (dimensionless) responses in alpha amplitude (top row) and alpha frequency (bottom row), induced by 50% modulation of the gains ((A) and (C)) and modulation of the phases by $\pm\pi/4$ rad ((B) and (D)) of the three system circuits (blue, green, and red correspond to the feedforward, thalamo-cortico-thalamic, and intra-cortical circuits, respectively).

Table 3
Alpha responses induced by gain and phase modulations of system circuits. ΔA and ΔF denote relative responses in alpha amplitude and frequency, respectively. pos. and neg. refer to positively and negatively correlated responses, respectively.

	ΔA	ΔF	Type
Feedforward gain (G_X)	+	0	
Cortico-thalamo-cortical gain (G_Y)	−	+	neg.
Intra-cortical gain (G_Z)	+	+	pos.
Feedforward phase (ϕ_X)	0	0	
Cortico-thalamo-cortical phase (ϕ_Y)	+	+	pos.
Intra-cortical phase (ϕ_Z)	+	−	neg.

neuronal populations and we vary p_- in the direction that increases the firing-rates of inhibitory neuronal populations. Also, since variation of synaptic rate-constants and efficacies have opposite effects on synaptic impacts and since alpha responses upon changes in synaptic parameters are effectively mediated through changes in synaptic impacts, we only consider variation of synaptic efficacies. Fig. 8(A) displays the alpha responses caused by 2% variations of p_+. Observe that for all parameters, both alpha amplitude and frequency increase, relative to baseline. Figs. 8(B) and (C) illustrate the alpha response induced by an increase in the efficacy of inter-pyramidal synaptic transmission ρ_{ee}. As Fig. 9 shows, variations of p_- lead to decreased alpha amplitude and frequency, relative to baseline. Taken together, Figs. 8 and 9 show that positive and negative alpha responses reflect, respectively, increased and decreased cortical activation.

Consideration of the gains and phases of X, Y, and Z, shows that the same modulations in the feedforward, cortico-thalamo-cortical, and intra-cortical circuits underly positive alpha responses and that the same in true for negative alpha responses. Fig. 10 shows representative modulations underlying positive alpha responses, in this case induced by an increase of 2% of the synaptic efficacy ρ_{ee}. Fig. 10(A) shows that G_x and G_Z increase, while G_Y decreases, which all contribute to the observed increase in alpha amplitude as can be seen from Fig. 7(A). Furthermore, the modulations of the circuit phases are so modest that their effect on alpha amplitude can be neglected. Thus, to a first approximation, the increased alpha amplitude reflects modulations in the gains of the different system circuits. In contrast, while the increase in G_Z contributes to the observed increase in alpha frequency, the contribution of the decrease in ϕ_Z is much larger, which shows that ϕ_Z determines the positive alpha frequency response. Physiologically, this means that the observed increase in alpha frequency mainly reflects a decreased delay in the intra-cortical circuit at alpha baseline frequency.

Benzodiazepine-induced alpha responses

Benzodiazepines such as diazepam, lorazepam, and clonazepam form a class of psychoactive drugs that possess sedative, hypnotic, anxiolytic, and anti-convulsive properties. They are known to modulate the properties of spontaneous human EEG oscillations in different frequency bands, including the delta, alpha, and beta bands (Buchsbaum et al., 1985; Kuizenga et al., 2001). Concerning alpha oscillations, when administered in low doses, benzodiazepines induce decreases in alpha amplitude as well as frequency (Frost et al., 1973). In this section we incorporate the pharmacological action of benzodiazepines in the thalamo-cortical model of EEG generation (Robinson et al., 2002), demonstrate that the model is able to reproduce the experimentally observed alpha responses, and characterize the underlying modulations of the resonances of the feedforward, cortico-thalamo-cortical, and intra-cortical circuits.

The main targets of benzodiazepines within the central nervous system are γ -aminobutyric receptors of type A ($GABA_A$). Specifically, benzodiazepines are a positive allosteric modulator of $GABA_A$ receptors and act by enhancing the affinity of GABA, thereby increasing the maximal chloride conductance (Rogawski and Löscher, 2004; Treiman, 2001). The GABA-ergic system however, comprises over a dozen $GABA_A$ receptor subtypes (McKernan, 1996), distributed throughout the brain, in particular cortical and thalamic tissue (Kandel et al., 2000), with largely

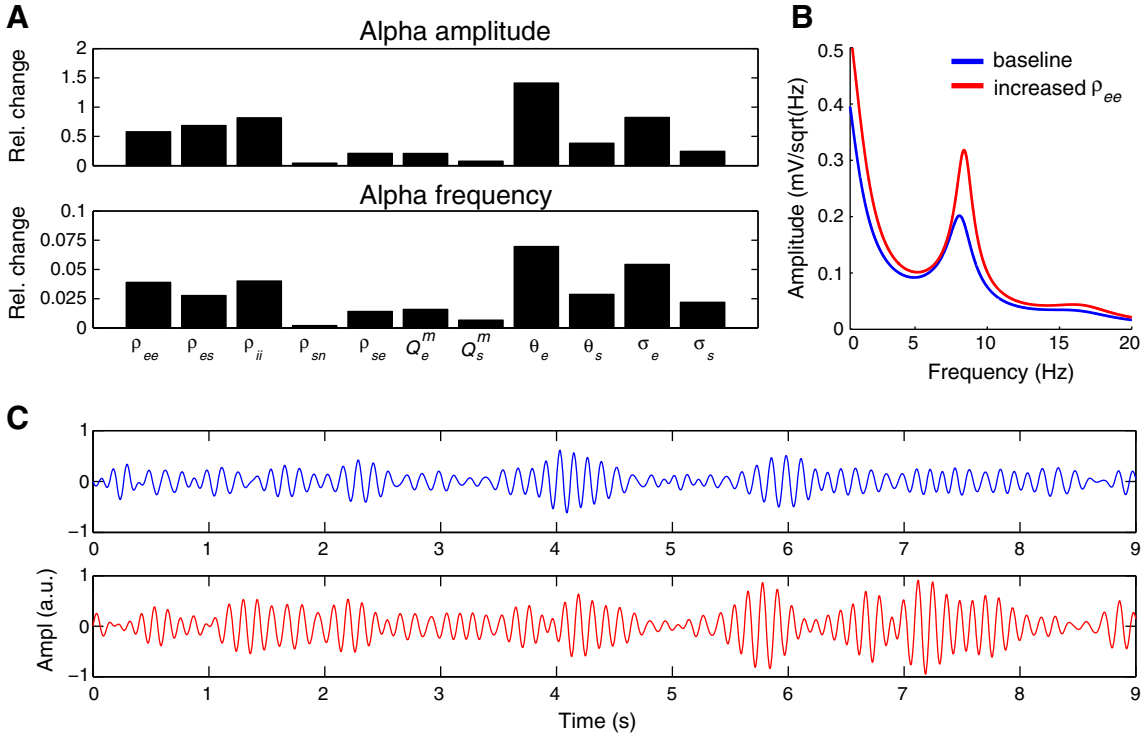

Fig. 8. Alpha responses induced by increased cortical activation. (A) Relative responses in alpha amplitude (top row) and frequency (bottom row) induced by 2% changes in p_+. (B) Theoretical EEG power spectra in baseline (blue) and resulting from a 2% increase in the efficacy of inter-pyramidal synaptic transmission (ρ_{ee}). (C) Simulated EEG time-series corresponding to the spectra in (B). The time-series were bandpass-filtered in the band of 6–10 Hz to highlight alpha activity.

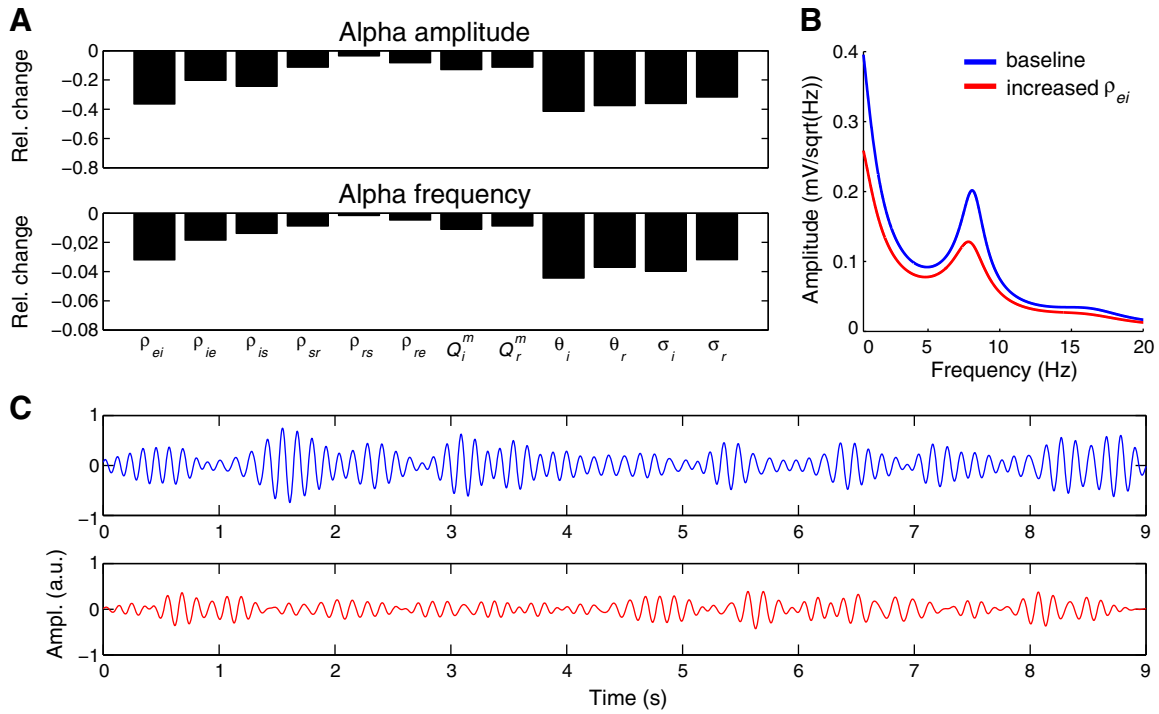

Fig. 9. Alpha responses induced by increased cortical deactivation. (A) Relative responses in alpha amplitude (top row) and frequency (bottom row) induced by 2% changes in p_{-}. (B) Theoretical EEG power spectra in baseline (blue) and resulting from a 2% increase in the efficacy of inter-pyramidal synaptic transmission (ρ_{ee}). (C) Simulated EEG time-series corresponding to the spectra in (B). The time-series were bandpass-filtered in the band of 6–10 Hz to highlight alpha activity.

unknown regional and cellular distributions (Sieghart and Sperk, 2002). In the thalamo-cortical meanfield model used in this study (Robinson et al., 2002), three different subtypes of $GABA_A$ receptors are modeled explicitly, namely those located on the dendrites of cortical inhibitory neurons, cortical pyramidal neurons, and thalamo-cortical relay neurons (see Fig. 1). The synaptic efficacies of these receptor subtypes are given by the parameters ρ_{ii}, ρ_{ei}, and ρ_{sr}, respectively. Taking into account the known pharmacology of benzodiazepines and in line with Liley et al. (2003), we model the action of benzodiazepines by

$$\rho_{ki} \mapsto (1 + \epsilon_k(\xi - 1))\rho_{ki}, \tag{17}$$

for $k = i,e,s$, where ϵ_k models the differential affinities of benzodiazepines for the different $GABA_A$ receptor subtypes and $\xi \geq 1$ models benzodiazepine concentration ($\xi = 1$ corresponds to baseline). We set $\epsilon_i = 1$ so that ϵ_e and ϵ_s model the differential affinities of benzodiazepine for $GABA_A$ receptors located on cortical pyramidal neurons and thalamo-cortical relay neurons, respectively, relative to its differential affinity for the $GABA_A$ receptors located on the dendrites of cortical inhibitory neurons. Thus, $\epsilon_e = 1$ corresponds to an equal affinity of benzodiazepines for $GABA_A$ receptors located on cortical pyramidal neurons and cortical inhibitory neurons and $\epsilon_s = 0$ corresponds to complete insensitivity of benzodiazepines to $GABA_A$ receptors located on thalamo-cortical relay neurons. Since the induced alpha response predominantly depends on the value of ϵ_e, we set $\epsilon_s = \epsilon_e$ and consider the alpha response properties as a function of ϵ_e.

Figs. 11(A) and (B) display the responses in alpha amplitude and frequency, relative to baseline, as a function of ϵ_e. They show that, depending on the value of ϵ_e, the thalamo-cortical system can respond in three qualitatively different ways. Specifically, for low values of ϵ_e, both alpha amplitude and frequency increase, for intermediate values of ϵ_e, alpha amplitude increases while alpha frequency decreases, and for high values of ϵ_e, both alpha amplitude and frequency decrease. Thus, the experimentally observed decreases in alpha amplitude and frequency upon administration of benzodiazepines (Frost et al., 1973) are reproduced only when ϵ_e is sufficiently larger than 1 (about 1.08). Physiologically, this means that benzodiazepines are predicted to possess a higher differential affinity for $GABA_A$ receptor subtypes located on cortical pyramidal neurons than for $GABA_A$ receptor subtypes located on cortical inhibitory neurons. Figs. 11(C) and (D) display benzodiazepine-induced modulations in the feedforward, cortico-thalamo-cortical and intra-cortical circuits underlying negative alpha responses ($\epsilon_e = 1.2$). Using the results summarized in Fig. 7, this shows that the benzodiazepine-induced increase in alpha amplitude reflects modulations of the gains of all three system circuits and that the benzodiazepine-induced decrease in alpha frequency predominantly reflects an increase in the phase ϕ_Z of the intra-cortical circuit.

Discussion

In this study we used a meanfield model of the thalamo-cortical system (Rennie et al., 2002; Robinson et al., 2001, 2002) to obtain a fundamental understanding of the thalamo-cortical mechanisms underlying alpha responses observed in human EEG experiments. Our main result is that alpha responses effectively depend on the modulations of the resonance properties of the feedforward, cortico-thalamo-cortical, and intra-cortical circuits, which are characterized by frequency-independent gains and phases. Physiologically, the gains and phases quantify the extent to which incoming oscillations at the alpha baseline frequency are attenuated and delayed, respectively, within these circuits. We have established that modulations of the gains and phases of each of these circuits have a distinct effect on the amplitude and frequency of EEG alpha oscillations. In particular, the frequency of ongoing EEG alpha oscillations is most sensitive to the time-delay within the intra-cortical circuitry, which highlights the role of intrinsic cortical feedback in determining alpha frequency. Furthermore, by investigating the effect of synaptic and intrinsic neuronal properties, we have shown that the induced alpha responses reflect the activation level of cortical tissue. This is in line with the alpha-suppression hypothesis that states

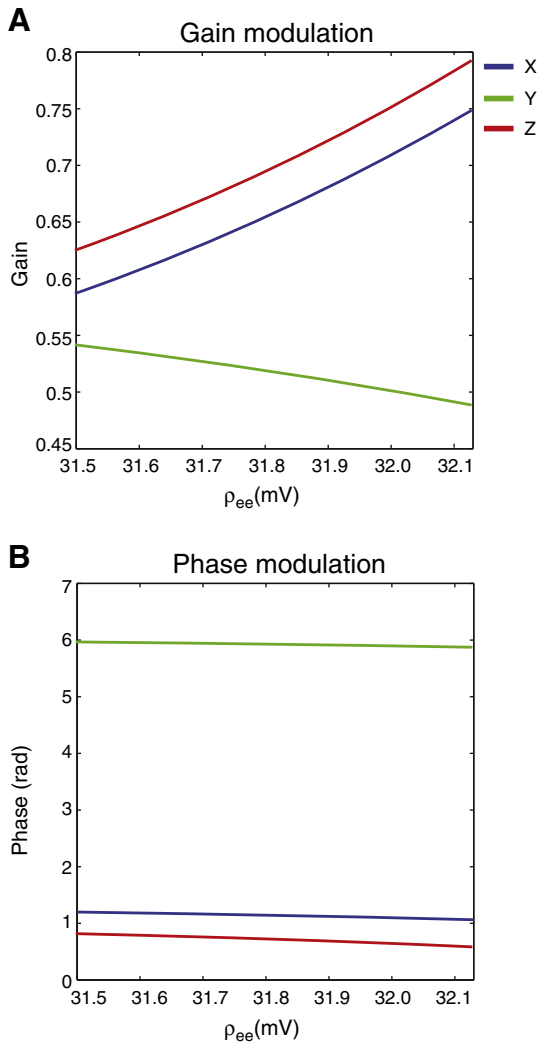

Fig. 10. Parameter-induced resonance modulations. Shown are the modulations in the gains (A) and phases (B) of alpha baseline frequency of the feedforward (blue lines), cortico-thalamo-cortical (green lines), and intra-cortical (red lines) circuits, due to a 2% increase in the efficacy of inter-pyramidal synaptic transmission (ρ_{ee}).

that alpha activity serves to selectively inhibit cortical regions during cognitive processing tasks (Klimesch et al., 2007). The increased firing-rates of cortical pyramidal neurons associated with increased alpha amplitude and frequency are also plausible from a physiological point of view. The rationale behind this is that increased amplitude reflects a larger number of neurons participating in the generation of the oscillations and increased frequency reduces the temporal spacing of spikes underlying the oscillations, hence both increase the average firing-rate within the neuronal population underlying the oscillations.

Regarding the physiological interpretation of experimental studies on alpha responses, a natural question is whether the modulations of the system circuits can be inferred directly from recorded EEG data. This inverse problem is ill-posed, since, in general, alpha responses are likely to result from simultaneous modulations of the resonance properties of the feedforward, cortico-thalamo-cortical, and intra-cortical circuits. By imposing certain a priori physiological restrictions however, it is possible to estimate the excitabilities within the different loop structures comprising the thalamo-cortical system directly from the broadband EEG spectrum (Robinson et al., 2004; Rowe et al., 2004) and this approach could also be adopted to estimate gain and phase modulations. This approach has already been successfully applied to broadband EEG power changes observed in subjects diagnosed with ADHD (Rowe et al., 2005). To arrive at a completely general estimation procedure, there are at least two ways that seem promising. First, in the thalamo-cortical model, the resonance-modulations of the different circuits are not independent but are restricted by the changes in the equilibrium firing rates of the different neuron types. Thus, by imposing the relations between the equilibrium firing-rates of the different neuron types as expressed by their equilibrium equations (see Appendix D) one might be able to render the inverse problem well-posed. Second, the approach taken in Robinson et al. (2004) and Rowe et al. (2004) only uses the power spectrum of the recorded EEG data hence discards their temporal structure. An alternative approach therefore, is to incorporate the data's temporal structure in the estimation procedure, for example by making use of Bayesian inference techniques as proposed in Golightly and Wilkinson (2008). Development of general estimation techniques will enable to determine and quantify the changes in the functionality of the thalamo-cortical system that underly alpha responses in specific experiments.

Despite the difficulties involved in determining the resonance-modulations underlying alpha responses observed in specific experiments, the findings described in his study qualitatively agree with experimental observations in several respects. First, the model can reproduce both positively as well as negatively correlated alpha responses, which shows that the model is flexible enough to capture the kinds to alpha responses encountered in experiments (Banquet, 1973; Feshchenko et al., 2004; Volavka et al., 1973). Second, one of the characteristics of the alpha responses generated by the thalamo-cortical model used in this study is that changes in alpha frequency are much smaller than changes in alpha amplitude. This is in agreement with experimental observations, where alpha peak-frequencies across conditions typically differ by less than 20% (Banquet, 1973; Domino et al., 2009; Feshchenko et al., 2004; Kostyunina and Kulikov, 1996; Moretti, 2004; Roth, 1991; Volavka et al., 1973), while alpha peak-amplitudes can show much larger differences (Banquet, 1973; Jensen et al., 2002; Klimesch et al., 2007; Knyazev et al., 2004; Koehler et al., 2009). Third, resonance-modulations induce mono-phasic alpha responses, both in amplitude as well as in frequency. This might explain why in experiments, alpha amplitude and frequency typically display linear correlations with cognitive (Jensen et al., 2002; Knyazev et al., 2004), neuropsychological (Kuskowski et al., 1993), pharmacological (Dafters et al., 1999; Feshchenko et al., 2004), and emotional (Knyazev et al., 2004) indices. These results motivate further use of the currently used thalamo-cortical model for EEG generation in the study on mechanisms underlying alpha responses.

In this study we have illustrated how the presented methodology might be applied to elucidate the mechanisms underlying alpha responses in a concrete experimental protocol, namely that of benzodiazepine-induced responses (Frost et al., 1973). To reproduce the experimentally observed responses, which comprise a decrease in both alpha amplitude as well as peak-frequency, we incorporated the pharmacological action of benzodiazepines into the model. Specifically, since it is known that benzodiazepines are positive allosteric modulators of $GABA_A$ receptors (Rogawski and Löscher, 2004; Treiman, 2001) we modeled their action by differential increases in the GABAergic efficacies ρ_{ki} for $k \in \{e,i,s\}$. The methodology presented in the present study allows us to interpret the benzodiazepine-induced alpha responses in terms of resonance modulations within thalamo-cortical circuits and predicts that benzodiazepines possess a higher affinity for $GABA_A$ receptor subtypes on cortical pyramidal neurons than for $GABA_A$ receptor subtypes on cortical inhibitory neurons. Similarly as in the case of propofol-induced alpha responses (Hindriks and van Putten, 2012), the modeling suggests that changes in alpha amplitude and peak-frequency are triggered in local cortical circuits. Although this application illustrates the possible use of the methodology, a more thorough investigation of the effect of benzodiazepines on spontaneous alpha oscillations needs to consider the role of $GABA_A$ receptor subtypes located on thalamic reticular neurons (Browne et al., 2001), which are not incorporated into the current version of the model. Since the current model suggests benzodiazepine-induced decreases in alpha amplitude and frequency

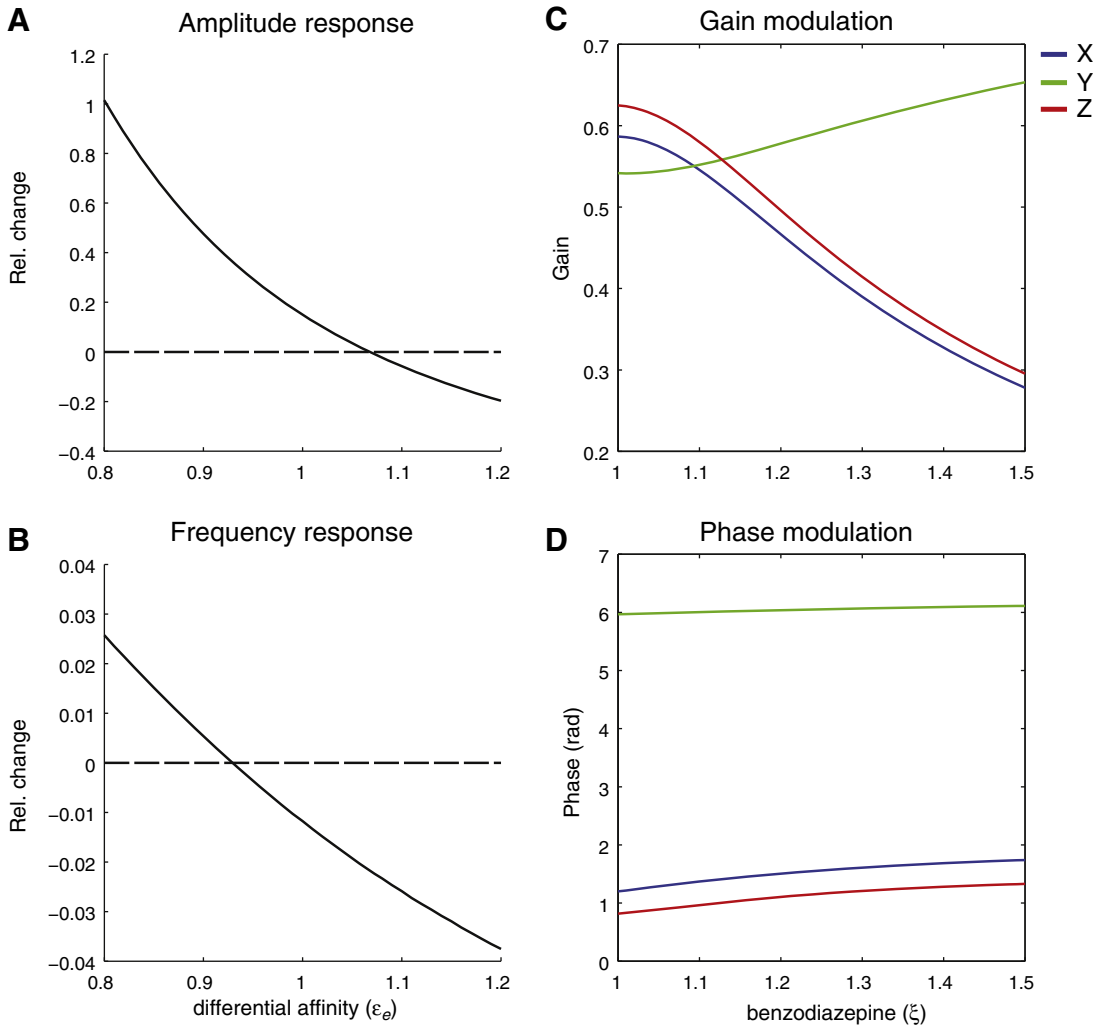

Fig. 11. Benzodiazepine-induced alpha responses. (A) and (B) display the response amplitude and frequency of spontaneous alpha oscillations, relative to baseline, respectively, as a function of the benzodiazepine affinity ε_e. The responses were obtained for a fixed benzodiazepine concentration of $\xi = 1.1$. (C) and (D) display the modulations in the gain and phase, respectively, of the feedforward, cortico-thalamo-cortical, and intra-cortical circuits, as a function of benzodiazepine concentration. The modulations were obtained by setting $\varepsilon_e = 1.2$.

to crucially depend on the pharmacological changes in cortical circuitry, we might expect that, in the case of extended thalamic synaptic organization, the effects of benzodiazepines will be qualitatively the same.

In this study, we have used baseline parameters for which the theoretical EEG power spectrum closely resembles experimentally measured spectra in human subjects during alert wakefulness (Robinson et al., 2002; Rowe et al., 2004). It is very well possible however, that different model parameters yield similar resting-state EEG spectra while the response of alpha oscillations to parameter variations is different than the ones reported in this study. Such a situation is known to exist for a cortical model of EEG generation (Bojak and Liley, 2005) in which it was found that the effect of anesthetic agents ongoing EEG alpha oscillations depended on the chosen baseline condition. Since different baselines within the model reflect different mental, behavioral, or arousal states of a single human subject or between subjects, the possible different response properties of modeled alpha might explain the variability of alpha responses (Banquet, 1973; Hindriks and van Putten, 2012), which is likely to be present in the majority of experimental studies but is often not reported since attention is focused on effects on the group level. However, exploration of differential alpha responses such as performed in Bojak and Liley (2005) is an interesting research direction since it has the potential to explain divergent experimental findings.

The analysis conducted in this study allows for a basic interpretation of experimentally alpha responses in terms of changes in the functional state of the thalamo-cortical system. There are however, several possible extensions that might enable a more complete picture to be drawn. The first extension concerns region-specific alpha responses and cortico-cortical coherence changes. Both in resting-state paradigms as well as in studies on evoked and induced alpha, one typically observes coordinated region-specific alpha responses (Banquet, 1973; Cantor et al., 1986; Dafters et al., 1999; Feshchenko et al., 2004; Jensen et al., 2002; Klimesch et al., 2007; Pfurtscheller et al., 1996) or coherence changes between cortical regions (Cantero et al., 1999; Dafters et al., 1999; Klimesch et al., 2007; Merrin and Floyd, 1989). Such observations are most likely caused by differential modulations within and between distinct thalamo-cortical modules. Mechanistic understanding of such observations therefore, requires the formulation and analysis of models comprised of coupled modules, for example as done in Drover et al. (2010) where the authors investigate EEG coherences that arise from reticular thalamic coupling between thalamo-cortical modules. The second extension concerns the physiological causes of modulations in the functionality of thalamo-cortical feedback loops. Although our study allows for an interpretation of alpha responses in terms of functional changes within thalamo-cortical feedback loops, the causes of these modulations are restricted to the synaptic and intrinsic neuronal physiology of thalamo-cortical tissue. However, in studies involving pharmacological manipulations (Dafters et al., 1999; Domino et al., 2009; Feshchenko et al., 2004; Lukas et al., 1990) or arousal and emotional

states (Banquet, 1973; Knyazev et al., 2004; Kostyunina and Kulikov, 1996), these modulations are known to be partially caused by changes in neuromodulatory systems, hence their study requires specific extensions of the currently used model, for example incorporation of acetylcholinergic pathways as done in Clearwater et al. (2007). Similarly, in sensory information processing paradigms, the relevant anatomy and physiology have to be included into the modeling as done for example, in the context of visual (Azizi et al., 1996) and auditory (Du and Jansen, 2011) evoked potentials or in the context of ERD in motor paradigms (Suffczynski et al., 2001). The models presented in these studies allow for an analysis similar as conducted in the current study, thereby providing generic insight into the mechanisms underlying alpha responses in specific experimental paradigms.

Appendix A. System equations

The average membrane potentials V_e, V_i, V_r, and V_s obey the following set of coupled equations:

$$V_e(t) = h_{ee} \otimes \phi_e(t) + h_{es} \otimes S_s(V_s(t-\tau/2)) + h_{ei} \otimes S_i(V_i(t)), \tag{18}$$

$$V_i(t) = h_{ie} \otimes \phi_e(t) + h_{is} \otimes S_s(V_s(t-\tau/2)) + h_{ii} \otimes S_i(V_i(t)), \tag{19}$$

$$V_s(t) = h_{sn} \otimes \phi_n(t) + h_{se} \otimes \phi_e(t-\tau/2) + h_{sr} \otimes S_r(V_r(t)), \tag{20}$$

$$V_r(t) = h_{rs} \otimes S_s(V_s)(t) + h_{re} \otimes \phi_e(t-\tau/2), \tag{21}$$

where t denotes time, $\otimes$ is the convolution operator, τ is the transmission delay between cortex and thalamus, and ϕ_n is non-specific input to thalamo-cortical relay neurons, which has the form $\phi_n = <\phi_n> + \sigma_n\xi(t)$, where $<\phi_n>$ denotes its mean value, $\xi(t)$ a unit-variance Gaussian white-noise process, and σ_n its standard deviation. Furthermore, the relation between V_e and ϕ_e is given by

$$\left[\left(\frac{1}{\gamma}\frac{\partial}{\partial t}+1\right)^2 - l^2\nabla^2\right]\phi_e(t) = Q_e(t), \tag{22}$$

where ϕ_e is the firing-rate from distant pyramidal populations coming in at time t, l the characteristic axonal length of cortical pyramidal neurons, and $\gamma = v/l$ is the cortical damping rate (Robinson et al., 1997). We set $\nabla^2 = 0$ which means that we restrict to spatially-homogeneous solutions of ϕ_e on the cortical sheet. Alternatively, by expressing the synaptic response functions as second-order differential operators, the above equations can be formulated as a set of coupled first-order ordinary differential equations (see for example Breakspear et al., 2006).

Appendix B. Theoretical EEG power spectrum

In this Appendix we derive the theoretical EEG power spectrum corresponding to the model Eqs. (18)–(22) of Appendix A. We note though, that this derivation is not completely novel since similar derivations have been carried out for different versions of the model (Rennie et al., 2002; Robinson et al., 2001, 2002; Rowe et al., 2004). For the currently used version of the model, we derive the EEG theoretical power spectrum by first rewriting Eqs. (18)–(22) of Appendix A in the frequency domain, giving

$$V_e = L_{ee}\phi_e + L_{es}Q_s e^{-i\omega\tau/2} + L_{ei}Q_i, \tag{23}$$

$$V_i = L_{ie}\phi_e + L_{is}Q_s e^{-i\omega\tau/2} + L_{ii}Q_i, \tag{24}$$

$$V_s = L_{sn}\phi_n + L_{se}\phi_e e^{-i\omega\tau/2} + L_{sr}Q_r, \tag{25}$$

$$V_r = L_{rs}Q_s + L_{re}\phi_e e^{-i\omega\tau/2}, \tag{26}$$

$$(1+i\omega/\gamma)^2\phi_e = Q_e. \tag{27}$$

By linearizing S about a stable steady-state V_k^* of V_k;

$$S(V_k) \approx S(V_k) + S'(V_k^*)V_k, \tag{28}$$

for $k \in \{e,i,r,s\}$ and by discarding constants, we can rewrite Eqs. (23)–(27) in the frequency domain as

$$(1+i\omega/\gamma)^2\phi_e = \delta_{ee}\phi_e + \delta_{es}Q_s e^{-i\omega\tau/2} + \delta_{ei}Q_i, \tag{29}$$

$$Q_i = \delta_{ie}\phi_e + \delta_{is}Q_s e^{-i\omega\tau/2} + \delta_{ii}Q_i, \tag{30}$$

$$Q_s = \delta_{sn}\phi_n + \delta_{se}\phi_e e^{-i\omega\tau/2} + \delta_{sr}Q_r, \tag{31}$$

$$Q_r = \delta_{rs}Q_s + \delta_{re}\phi_e e^{-i\omega\tau/2}. \tag{32}$$

We now substitute Eq. (32) into Eq. (31) and isolate Q_s, giving

$$Q_s = \frac{\delta_{sn}\phi_n + (\delta_{se}+\delta_{sre})\phi_e e^{-i\omega\tau/2}}{1-\delta_{srs}}. \tag{33}$$

By substituting Eq. (33) into Eq. (30) and isolating Q_i we obtain

$$Q_i = \frac{\delta_{ie}(1-\delta_{srs}) + (\delta_{ise}+\delta_{isre})e^{-i\omega\tau}}{(1-\delta_{ii})(1-\delta_{srs})}\phi_e + \frac{\delta_{isn}e^{-i\omega\tau/2}}{(1-\delta_{ii})(1-\delta_{srs})}\phi_n.$$

By substituting the expressions for Q_s and Q_i into Eq. (29) and re-arranging terms, we obtain

$$\left[2i\omega/\gamma - \omega^2/\gamma^2 + \mathrm{Y}(\omega)\right]\phi_e = \mathrm{X}(\omega)e^{-i\omega\tau/2}\phi_n + \mathrm{Z}(\omega)e^{-i\omega\tau}\phi_e, \tag{34}$$

where $\mathrm{X}(\omega)$,$\mathrm{Y}(\omega)$, and $\mathrm{Z}(\omega)$, are defined by Eqs. (9)–(11) in the main text. Eq. (11) can be re-written to give the transfer function from ϕ_n to ϕ_e:

$$\frac{\phi_e}{\phi_n} = \frac{\mathrm{X}(\omega)e^{-i\omega\tau/2}}{2i\omega/\gamma - \omega^2/\gamma^2 + \mathrm{Y}(\omega) - \mathrm{Z}(\omega)e^{-i\omega\tau}}. \tag{35}$$

Since the EEG power spectrum $\mathrm{P}_{\mathrm{EEG}}(\omega)$ is defined as

$$\mathrm{P}_{\mathrm{EEG}}(\omega) = \phi_n^2\left|\frac{\phi_e}{\phi_n}\right|^2, \tag{36}$$

assuming the afferent input ϕ_n to be white-noise; $\phi_n = \sigma_n^2$, gives the equation for the EEG power spectrum:

$$\mathrm{P}_{\mathrm{EEG}}(\omega) = \frac{\sigma_n^2|\mathrm{X}(\omega)|^2}{\left|2i\omega/\gamma - \omega^2/\gamma^2 + \mathrm{Y}(\omega) - \mathrm{Z}(\omega)e^{-i\omega\tau}\right|^2}. \tag{37}$$

Appendix C. Parametrization of the instability boundary

In this section we express the equation that characterizes the boundary of the linear instability region in terms of the variables Y and Z. The motivation for this is to connect these variables to the coordinates derived in Robinson et al. (2002) to parameterize the same equation in a more specific version of the thalamo-cortical model and in the low-frequency limit. The variable X is not related to any of these coordinates since it does not affect model stability. Throughout our derivation we use the notation introduced in this study, which differs slightly from that used in Robinson et al. (2002). In Robinson et al. (2002), the coordinates are derived under the assumption that $\rho_{ik} = \rho_{ek}$ for $k \in \{e,i,r,s\}$ (random connectivity) and by assuming that all synaptic types have the same dynamics ($\alpha_{kl} = \alpha$ and $\beta_{kl} = \beta$). Under

these assumptions, the linear stability boundary is characterized by the equation

$$2i\omega/\gamma - \omega^2/\gamma^2 + \mathrm{Y}(\omega) - \mathrm{Z}(\omega)e^{-i\omega\tau} = 0, \tag{38}$$

where Y and Z are now reduced to

$$\mathrm{Y}(\omega) = 1 - \frac{\delta_{ee}}{1-\delta_{ei}}, \tag{39}$$

and

$$\mathrm{Z}(\omega) = \frac{\delta_{ese} + \delta_{esre}}{(1-\delta_{srs})(1-\delta_{ei})}. \tag{40}$$

Following Robinson et al. (2002), in the low-frequency limit, we can substitute $L_{kl} \approx L_{kl}(0) \equiv L^0_{kl}$ in Eqs. (39), and (40), except in the term $1-\delta_{srs}$. By denoting $G_{kl} = \epsilon_l L^0_{kl}$ we obtain

$$\mathrm{Y}(\omega) = 1 - \frac{G_{ee}}{1-G_{ei}}, \tag{41}$$

and

$$\mathrm{Z}(\omega) = \frac{G_{ese} + G_{esre}}{(1-\epsilon_r\epsilon_s L(\omega)^2)(1-G_{ei}).} \tag{42}$$

Rewriting Eq. (38) in the form of (Robinson et al., 2002) (page 4, Eq. (12)) gives

$$(1 + i\omega/\gamma)^2 - (1-\mathrm{Y}) - \mathrm{Z}(\omega)e^{-i\omega\tau} = 0, \tag{43}$$

from which it follows that the coordinates x and y in Robinson et al. (2002) are related to Y and Z, respectively, through

$$x = 1 - Y = \frac{G_{ee}}{1-G_{ei}} \tag{44}$$

and

$$y = \mathrm{Z}(\omega) - \epsilon_s \frac{\epsilon_r L(\omega)^2}{1-G_{srs}} = \frac{G_{ese} + G_{esre}}{(1-G_{srs})(1-G_{ei})}, \tag{45}$$

which relate to intra-cortical and thalamo-cortico-thalamic instability, respectively. The third coordinate z used in Robinson et al. (2002) to parameterize the boundary of linear instability is proportional to $-G_{srs}$ and relates to intra-thalamic instability. Note that x, y, and z are independent of frequency, which makes them suitable to map the instability boundary as done in Robinson et al. (2002).

Appendix D. Equilibrium equations

For a time-independent afferent input $\phi_n(x,t) = q$, the firing rates (Q_e,Q_i,Q_s,Q_r) remain in an equilibrium state $(Q^*_e,Q^*_i,Q^*_s,Q^*_r)$. Equations for these steady-states can be derived in a similar way as done in Robinson et al. (1997). Specifically, from Eqs. (18)–(22) of Appendix A, we deduce that the equilibrium firing-rates satisfy

$$\begin{aligned}
S^{-1}(Q^*_e) &= h_{ee} \otimes Q^*_e + h_{es} \otimes Q^*_s + h_{ei} \otimes Q^*_i,\\
S^{-1}(Q^*_i) &= h_{ie} \otimes Q^*_e + h_{is} \otimes Q^*_s + h_{ii} \otimes Q^*_i,\\
S^{-1}(Q^*_s) &= h_{sn} \otimes \phi_n + h_{se} \otimes Q^*_e + h_{sr} \otimes Q^*_r,\\
S^{-1}(Q^*_r) &= h_{rs} \otimes Q^*_s + h_{re} \otimes Q^*_e,
\end{aligned}$$

where we have used that $Q^*_k = S(V^*_k)$, where V^*_k denotes the equilibrium value of V_k for $k \in \{e,i,s,r\}$. Since the terms Q^*_k are time-independent, the convolutions $h \otimes Q^*_l$ reduce to

$$h \otimes Q^*_k = Q^*_k \int_0^\infty h_{kl}(t)dt = Q^*_l \lambda_{kl},$$

which yields the equilibrium equations for the firing-rates

$$\begin{aligned}
S^{-1}(Q^*_e) &= \lambda_{ee}Q^*_e + \lambda_{ei}Q^*_i + \lambda_{es}Q^*_s,\\
S^{-1}(Q^*_i) &= \lambda_{ie}Q^*_e + \lambda_{ii}Q^*_i + \lambda_{is}Q^*_s,\\
S^{-1}(Q^*_s) &= \lambda_{sn}Q_n + \lambda_{se}Q^*_e + \lambda_{sr}Q^*_r,\\
S^{-1}(Q^*_r) &= \lambda_{rs}Q^*_s + \lambda_{re}Q^*_e.
\end{aligned}$$

References

Azizi, S., Ogmen, H., Jansen, B.H., 1996. A unified analysis of alpha rhythm, fast synchronized oscillations, and flash visual evoked potentials. Neural Netw. 9 (2), 223–242.

Banquet, J.P., 1973. Spectral analysis of the EEG in meditation. Electroencephalogr. Clin. Neurophysiol. 35 (2), 143–151.

Berger, H., 1929. Uber das Elektrenkephalogramm des Menschen. Eur. Arch. Psychiatry Clin. Neurosci. 278, 1929.

Bojak, I., Liley, D., 2005. Modeling the effects of anesthesia on the electroencephalogram. Phys. Rev. E 71 (4), 1–22 (April).

Breakspear, M., Roberts, J.A., Terry, J.R., Rodrigues, S., Mahant, N., Robinson, P.A., 2006. A unifying explanation of primary generalized seizures through nonlinear brain modeling and bifurcation analysis. Cereb. Cortex 16 (9), 1296–1313 (New York, N.Y.: 1991 September).

Browne, S.H., Kang, J., Akk, G., Chiang, L.W., Schulman, H., Huguenard, J.R., Prince, D.A., 2001. Kinetic and pharmacological properties of GABA A receptors in single thalamic neurons and GABA A subunit expression. J. Neurophysiol. 86, 2312–2322.

Buchsbaum, M.S., Hazlett, E., Sicotte, N., Stein, M., Wu, J., Zetin, M., 1985. Topographic EEG changes with benzodiazepine administration in generalized anxiety disorder. Biol. Psychiatry 20 (8), 832–836 (August).

Cantero, J.L., Atienza, M., Salas, R.M., 1999. Alpha EEG coherence in different brain states: an electrophysiological index of the arousal level in human subjects. Neurosci. Lett. 271 (3), 167–170 (August).

Cantor, D.S., Thatcher, R.W., Hrybyk, M., Kaye, H., 1986. Computerized EEG analyses of autistic children. J. Autism Dev. Disord. 16 (2), 169–187 (June).

Clearwater, J.M., Rennie, C.J., Robinson, P.A., 2007. Mean field model of acetylcholine mediated dynamics in the cerebral cortex. Biol. Cybern. 97 (5–6), 449–460 (December).

Dafters, R.I., Duffy, F., O'Donnell, P.J., Bouquet, C., 1999. Level of use of 3,4-methylenedioxymethamphetamine (MDMA or Ecstasy) in humans correlates with EEG power and coherence. Psychopharmacology 145 (1), 82–90 (July).

Domino, E.F., Ni, L., Thompson, M., Zhang, H., Shikata, H., Hiromi, F., Sakaki, T., Ohya, I., 2009. Tobacco smoking produces widespread dominant brain wave alpha frequency increases. Int. J. Psychophysiol. 74 (3), 192–198.

Drover, J.D., Schiff, N.D., Victor, J.D., 2010. Dynamics of coupled thalamocortical modules. J. Comput. Neurosci. 28 (3), 605–616 (June).

Du, X., Jansen, B.H., 2011. A neural network model of normal and abnormal auditory information processing. Neural Netw. 24, 568–574.

Feshchenko, V.A., Veselis, R.A., Reinsel, R.A., 2004. Propofol-induced alpha rhythm. Neuropsychobiology 50 (3), 257–266 (January).

Flor-Henry, P., Koles, Z.J., 1984. Statistical quantitative EEG studies of depression, mania, schizophrenia and normals. Biol. Psychol. 19 (3–4), 257–279.

Frost Jr., J.D., Carrie, J.R.G., Borda, R.P., Kellaway, P., 1973. The effects of dalmane (flurazepam hydrochloride) on human EEG characteristics. Electroencephalogr. Clin. Neurophysiol. 34 (2), 171–175.

Goldman, R.I., Stern, J.M., Engel, J., Cohen, M.S., 2002. Simultaneous EEG and fMRI of the alpha rhythm. Neuroreport 13 (18), 2487–2492 (December).

Golightly, A., Wilkinson, D.J., 2008. Bayesian inference for nonlinear multivariate diffusion models observed with error. Comput. Stat. Data Anal. 52 (3), 1674–1693 (January).

Gonçalves, S.I., de Munck, J.C., Pouwels, P.J.W., Schoonhoven, R., Kuijer, J.P.A., Maurits, N.M., Hoogduin, J.M., Van Someren, E.J.W., Heethaar, R.M., Lopes da Silva, F.H., 2006. Correlating the alpha rhythm to BOLD using simultaneous EEG/fMRI: inter-subject variability. NeuroImage 30 (1), 203–213 (March).

Gotlib, I.H., 1998. EEG alpha asymmetry, depression, and cognitive functioning. Cogn. Emot. 12 (3), 449–478.

Hindriks, R., van Putten, M.J.A.M., 2012. Meanfield modeling of propofol-induced changes in spontaneous EEG rhythms. NeuroImage 60 (4), 2323–2334 (February).

Hindriks, R., Bijma, F., van Dijk, B.W., van der Werf, Y.D., van Someren, E.J.W., van der Vaart, A.W., 2011. Dynamics underlying spontaneous human alpha oscillations: a data-driven approach. NeuroImage 57 (2), 440–451 (July).

Hummel, F., Andres, F., Altenmüller, E., Dichgans, J., Gerloff, C., 2002. Inhibitory control of acquired motor programmes in the human brain. Brain 125 (Pt 2), 404–420 (February).

Jensen, O., Gelfand, J., Kounios, J., Lisman, J., 2002. Oscillations in the alpha band (9–12 Hz) increase with memory load during retention in a short-term memory task. Cereb. Cortex 12 (8), 877–882 (New York, N.Y.: 1991 August).

Kandel, E.R., Schwartz, J.H., Jessell, T.M., 2000. Principles of neuroscience.

Klimesch, W., Doppelmayr, M., Russegger, H., Pachinger, T., Schwaiger, J., 1998. Induced alpha band power changes in the human EEG and attention. Neurosci. Lett. 244 (2), 73–76 (March).

Klimesch, Wolfgang, Sauseng, Paul, Hanslmayr, Simon, 2007. EEG alpha oscillations: the inhibition-timing hypothesis. Brain Res. Rev. 53 (1), 63–88 (January).

Knyazev, G.G., Savostyanov, A.N., Levin, E.A., 2004. Alpha oscillations as a correlate of trait anxiety. Int. J. Psychophysiol. 53 (2), 147–160 (July).

Koehler, S., Lauer, P., Schreppel, T., Jacob, C., Heine, M., Boreatti-Hümmer, A., Fallgatter, A.J., Herrmann, M.J., 2009. Increased EEG power density in alpha and theta bands in

adult ADHD patients. J. Neural Transm. 116 (1), 97–104 (Vienna, Austria: 1996 January).
Kostyunina, M.B., Kulikov, M.A., 1996. Frequency characteristics of EEG spectra in the emotions. Neurosci. Behav. Physiol. 26 (4), 340–343.
Kuizenga, K., Wierda, J.M.K.H., Kalkman, C.J., 2001. Biphasic EEG changes in relation to loss of consciousness during induction with thiopental, propofol, etomidate, midazolam or sevoflurane. Br. J. Anaesth. 86 (3), 354–360.
Kuskowski, M.A., Mortimer, J.A., Morley, G.K., Malone, S.M., Okaya, A.J., 1993. Rate of cognitive decline in Alzheimer's disease is associated with EEG alpha power. Biol. Psychiatry 33 (8–9), 659–662 (April).
Larson, C.L., Davidson, R.J., Abercrombie, H.C., Ward, R.T., Schaefer, S.M., Jackson, D.C., Holden, J.E., Perlman, S.B., 1998. Relations between PET-derived measures of thalamic glucose metabolism and EEG alpha power. Psychopharmacologia 35, 162–169.
Liley, D.T.J., Cadusch, P.J., 2002. A spatially continuous mean field theory of electrocortical activity. Netw. Comput. Neural Syst. 13 (1), 67–113 (February).
Liley, D., Cadusch, P., Gray, M., Nathan, P., 2003. Drug-induced modification of the system properties associated with spontaneous human electroencephalographic activity. Phys. Rev. E 68 (5), 1–15 (November).
Lodder, S.S., van Putten, M.J.A.M., 2011. Automated EEG analysis: characterizing the posterior dominant rhythm. J. Neurosci. Methods 200 (1), 86–93 (August).
Lopes da Silva, F.H., Hoeks, A., Smits, H., Zetterberg, L.H., 1974. Model of brain rhythmic activity. Kybernetic 15, 27–37.
Lukas, S.E., Mendelson, J.H., Kouri, E., Bolduc, M., Amass, L., 1990. Ethanol-induced alterations in EEG alpha activity and apparent source of the auditory P300 evoked response potential. Alcohol 7 (5), 471–477.
McKernan, R.M., 1996. Which GABAA-receptor subtypes really occur in the brain? Trends Neurosci. 19 (4), 139–143.
Merrin, E.L., Floyd, T.C., 1989. EEG coherence in unmedicated schizophrenic patients. Biol. Psychiatry 25, 60–66.
Merrin, E.L., Floyd, T.C., May 1996. Negative symptoms and EEG alpha in schizophrenia: a replication. Schizophr. Res. 19 (2–3), 151–161.
Moraes, W.A., Poyares, D.R., Guilleminault, C., Ramos, L.R., Bertolucci, P.H.F., Tufik, S., 2006. The effect of donepezil on sleep and REM sleep EEG in patients with Alzheimer disease: a double-blind placebo-controlled study. Sleep 29 (2), 199–205.
Moretti, D., 2004. Individual analysis of EEG frequency and band power in mild Alzheimer's disease. Clin. Neurophysiol. 115 (2), 299–308 (February).
Nordberg, A., Alafuzoff, I., Winblad, B., 1992. Nicotinic and muscarinic subtypes in the human brain: changes with aging and dementia. J. Neurosci. Res. 31 (1), 103–111.
Nunez, Paul L., 1974. The brain wave equation: a model for the EEG. Math. Biosci. 21, 279–297.
Nunez, P.L., 1989. Generation of human EEG by a combination of long and short range neocortical interactions. Brain Topogr. 1 (3), 199–215 (January).
Pfurtscheller, G., Stancák, A., Neuper, C., 1996. Event-related synchronization (ERS) in the alpha band—an electrophysiological correlate of cortical idling: a review. Int. J. Psychophysiol. 24 (1–2), 39–46 (November).
Rennie, C.J., Robinson, P.A., Wright, J.J., 2002. Unified neurophysical model of EEG spectra and evoked potentials. Biol. Cybern. 86 (6), 457–471 (June).
Robinson, P.A., Rennie, C.J., Wright, J.J., 1997. Propagation and stability of waves of electrical activity in the cerebral cortex. Phys. Rev. E 56 (1), 826 (July).
Robinson, P., Rennie, C., Wright, J., Bahramali, H., Gordon, E., Rowe, D., 2001. Prediction of electroencephalographic spectra from neurophysiology. Phys. Rev. E 63 (2), 19–33 (January).
Robinson, P., Rennie, C., Rowe, D., 2002. Dynamics of large-scale brain activity in normal arousal states and epileptic seizures. Phys. Rev. E 65 (4), 1–9 (April).
Robinson, P.A., Rennie, C.J., Rowe, D.L., O'Connor, S.C., 2004. Estimation of multiscale neurophysiologic parameters by electroencephalographic means. Hum. Brain Mapp. 23 (1), 53–72 (September).
Rogawski, M.A., Löscher, W., 2004. The neurobiology of antiepileptic drugs. Nat. Rev. Neurosci. 5 (7), 553–564 (July).
Roth, N., 1991. Effects of cigarette smoking upon frequencies of EEG alpha rhythm and finger tapping. Psychopharmacology 105, 186–190.
Rowe, D.L., Robinson, P.A., Rennie, C.J., 2004. Estimation of neurophysiological parameters from the waking EEG using a biophysical model of brain dynamics. J. Theor. Biol. 231 (3), 413–433 (December).
Rowe, D.L., Robinson, P.a., Gordon, E., 2005. Stimulant drug action in attention deficit hyperactivity disorder (ADHD): inference of neurophysiological mechanisms via quantitative modelling. J. Clin. Neurophysiol. 116 (2), 324–335 (February).
Sadato, N., Nakamura, S., Oohashi, T., Nishina, E., 1998. Neural networks for generation and suppression of alpha rhythm: a PET study. Neuroreport 9, 893–897.
Schreckenberger, M., Lange-Asschenfeldt, C., Lange-Asschenfeld, C., Lochmann, M., Mann, K., Siessmeier, T., Buchholz, H., Bartenstein, P., Gründer, G., 2004. The thalamus as the generator and modulator of EEG alpha rhythm: a combined PET/EEG study with lorazepam challenge in humans. NeuroImage 22 (2), 637–644 (June).
Sieghart, W., Sperk, G., 2002. Subunit composition, distribution and function of GABA_A receptor subtypes. Curr. Top. Med. Chem. 2, 795–816.
Stam, C.J., Pijn, J.P.M., Suffczynski, P., Lopes da Silva, F.H., 1999. Dynamics of the human alpha rhythm: evidence for non-linearity? Clin. Neurophysiol. 110 (10), 1801–1813 (October).
Steriade, M., Gloor, P., Llinas, R.R., Lopes Da Silva, F.H., Mesulam, M.M., 1990. Basic mechanisms of cerebral rhythmic activities. Electroencephalography 76, 418–508.
Suffczynski, P., Kalitzin, S., Pfurtscheller, G., Lopes da Silva, F.H., 2001. Computational model of thalamo-cortical networks: dynamical control of alpha rhythms in relation to focal attention. Int. J. Psychophysiol. 43 (1), 25–40 (December).
Treiman, D.M., 2001. GABAergic mechanisms in epilepsy. Epilepsia 42 (Suppl. 3(2)), 8–12 (January).
van Rotterdam, A., Lopes Da Silva, F.H., 1982. A model of the spatial–temporal characteristics of the alpha rhythm. Bull. Math. Biol. 44 (2), 283–305.
Volavka, J., Crown, P., Dornbush, R., Feldstein, S., Fink, M., 1973. EEG, heart rate and mood change ("high") after cannabis. Psychopharmacologia 32 (1), 11–25 (August).